https://doi.org/10.5194/egusphere-2025-1494
Preprint. Discussion started: 24 April 2025

Feeding strategy as a key driver of the bioaccumulation of MeHg in megabenthos

David J. Amptmeijer[1], Andrea Padilla[2], Sofia Modesti[2], Corinna Schrum[1, 2], and Johannes Bieser[1]

[1]Matter Transport and Ecosystem Dynamics, Helmhotz-Zentrum Hereon, Geesthacht, Germany
[2]Universität Hamburg, Institute for Marine Sciences, Mittelweg 177, 20146 Hamburg, Germany

Correspondence: David J. Amptmeijer (davidamptmeijer@gmail.com)

Abstract. The bioaccumulation of methylmercury (MeHg) in the marine food chain poses a neurotoxic risk to human health, especially through the consumption of seafood. Although MeHg bioaccumulation at higher trophic levels is relatively well understood, MeHg bioaccumulation at the base of the food web remains underexplored. Given the neurotoxic effects of methylmercury on human health, it is essential to understand the drivers of bioaccumulation at every level of the food chain. In this study, we incorporate six megabenthos functional groups into the ECOSMO marine end-to-end ecosystem model, coupled to the MERCY marine Hg cycling model. We investigated how various feeding strategies influence the bioaccumulation of both inorganic Hg (iHg) and MeHg in marine ecosystems. We show that the feeding strategy significantly influences bioaccumulation and correlates stronger with iHg than the trophic level and that suspension feeders have elevated iHg levels while filter feeders have higher MeHg values. Additionally, we show that the bioaccumulation of both iHg and MeHg can be accurately modeled solely based on feeding strategies in low trophic-level megabenthos. However, when modeling higher trophic levels, incorporating the allometric scaling law dramatically improves the model performance. These results demonstrate the need for a holistic approach in which iHg, MeHg, and trophic levels of organisms are evaluated at both high and low trophic levels to identify what food web structures drive high MeHg concentrations in seafood.

1 Introduction

Mercury (Hg) is a naturally occurring element. In addition to its natural occurrence, it is also emitted through various anthropogenic activities, such as the burning of fossil fuels, small-scale artisanal gold mining, and the production of cement and ferrous metals (Pacyna et al., 2006). These emissions have led to a threefold increase in environmental Hg compared to pre-anthropogenic levels.

When elemental Hg (Hg^0) is emitted, it can undergo long-range atmospheric transport. In this way, it can be transported on a global scale and deposited in the oceans, thus increasing Hg levels in the marine environment (Durnford et al., 2010). Marine Hg^0 is volatile and can return to the atmosphere or be oxidized into dissolved Hg (Hg^{2+}) (Sommar et al., 2020). This Hg^{2+} can be reduced back to volatile elemental Hg^0, or it can be methylated to dangerous neurotoxin methylmercury (MeHg), which occurs as monomethylmercury ($MMHg^+$) or dimethylmercury (DMHg) (Jensen and Jernelov, 1969; Lin et al., 2021). In this

https://doi.org/10.5194/egusphere-2025-1494
Preprint. Discussion started: 24 April 2025

paper, we will look at the bioaccumulation of three groups of Hg; total Hg (tHg) refers to all Hg, methylmercury (MeHg) refers to both $MMHg^+$ and DMHg, and inorganic Hg (iHg) refers to all Hg that is not MeHg.

There are two key processes involved in bioaccumulation: bioconcentration and biomagnification. Animals living in a polluted marine environment will absorb Hg directly from their environment; this is called bioconcentration. Both iHg and MeHg bioconcentrate. Since iHg is generally present in higher concentrations than MeHg, and its bioconcentration rate is higher, iHg is usually bioconcentrated faster than MeHg (Mason et al., 1996). The bioconcentration process can result in high Hg concentrations in organisms, and Hg volume concentration factors of up to 6.4E6 have been found (Schartup et al., 2018).

These already high Hg concentrations can be increased even further by biomagnification. Biomagnification refers to the increase in Hg with each successive trophic level in the food chain. The trophic transfer efficiency of MeHg (66-80%) is higher than that of iHg (7-46%), where MeHg accumulates at much higher levels in the food chain (Metian et al., 2020; Wang and Wong, 2003; Dutton and Fisher, 2012). These concentrations can become harmful to humans when consumed, and the consumption of MeHg-polluted seafood is the main risk of exposure to Hg for the average person (Sheehan et al., 2014).

The danger posed by the consumption of MeHg-contaminated seafood received a great deal of attention when more than 1000 people died in Japan in 1956 due to the consumption of contaminated seafood caught in Minamata Bay(Harada, 1995). In order to reduce the risk of further outbreaks of MeHg intoxications, the Minamata Convention on Mercury was founded. 151 countries have pledged to reduce their Hg emissions in support of the Minamata Convention and 128 countries have signed and ratified the convention. The global state of Hg as a pollutant and the effect of the Minamata Convention is periodically reviewed in the Minamata Convention Effectiveness Evaluation (Outridge et al., 2018).

While there is considerable understanding of MeHg bioaccumulation in high trophic levels, less is known about the bioaccumulation drivers at the base of the food web. The lower concentration of Hg at the base of the food web reduces the risk for humans, which is why these animals do not receive the same monitoring recommendations from the effectiveness evaluation of the Minamata Convention as fish, humans and wildlife (Evers et al., 2016). Furthermore, the effectiveness evaluation noted that the concentrations of Hg and MeHg in water and sediment are poorly correlated with the concentrations in biota. Thus, Hg levels in water and sediment do not receive the same monitoring recommendations.

Once Hg is bioconcentrated in primary producers, a strong link appears between the trophic level and Hg bioaccumulation (Madgett et al., 2021). This indicates that our understanding of Hg bioaccumulation in high trophic levels is greatly limited by our understanding of Hg bioaccumulation at the base of the food web.

Improving our understanding of bioaccumulation at the base of the food web is challenging, as the base of the food web is very complex (Silberberger et al., 2018). There are several distinct groups of megabenthos with different feeding strategies, such as bivalves that filter feed, lugworms that feed on sediment carbon particles, active hunters and scavengers such as shrimps and crabs, and sponges that feed on suspended dissolved material. These different feeding strategies allow them to exploit a variety of food sources, but different food sources can have different Hg concentrations, and Hg originating from different food sources can have different assimilation efficiencies. In this study, we hypothesize that the low-trophic-level biota feeding strategy has a significant impact on their Hg content.

https://doi.org/10.5194/egusphere-2025-1494
Preprint. Discussion started: 24 April 2025

We focus this study on the benthic food web. Although primary production in the North Sea can be highly variable due to factors such as wind (Daewel and Schrum, 2017), tidal mixing (Zhao et al., 2019) and nutrient availability (Richardson et al., 1998), primary production in coastal areas is generally dominated by pelagic phytoplankton, with the exception of extremely shallow areas that are dominated by benthic macroalgae (Krause-Jensen et al., 2012; Cibic et al., 2022). Especially in areas where pelagic phytoplankton dominate primary production, while the pelagic phytoplankton are available for consumption by megabenthos because of water column mixing, there is a strong coupling between the benthic and the pelagic, called the bentho-pelagic coupling. In these well-mixed areas, megabenthos can reach high biomass since food is abundant in several ways, resulting in megabenthos with different feeding strategies in the same ecosystem (Ghodrati Shojaei et al., 2016).

We hypothesize that the different feeding strategies of low-trophic-level megabenthos play an important role in creating the disconnect between Hg concentrations in the water and sediment and the concentrations at the base of the food web. We investigated whether the feeding strategy impacts bioaccumulation and hypothesized that feeding strategies influence the bioaccumulation of iHg and MeHg differently, contributing to the high variation in Hg levels at the base of the benthic food web.

To test our hypotheses, we employed two methods. First, we performed literature research in which we collected field observations of the content of tHg, MeHg, and iHg, the trophic level, and the megabenthos feeding strategy. We performed statistical analyses on this literature to see if patterns between bioaccumulation and feeding strategies exist in nature. Afterward, we conducted an in silico experiment in which megabenthos with various feeding strategies compete under physical drivers in idealized scenarios that are typical of megabenthos-rich coastal oceans. The megabenthos groups are designed to differ only in their feeding strategies to isolate this effect. This was done to verify whether we can reproduce the observed effects from our literature study in a fully coupled model. Finally, we used the model to quantify the role of the feeding strategy in the bioaccumulation of Hg and investigated whether it fully explains the observed differences or if other drivers need to be incorporated.

2 Materials and methods

2.1 Literature research and statistics

To compare the findings with the literature, we collected field studies measuring Hg in megabenthos. The studies we used are shown in the Table 5. We categorized the megabenthos into the same feeding categories, "deposit feeder", "filter feeder", "suspension feeder", "grazer" and "predator". To better look at the effect of the trophic level, we also added "primary producers" as the base of the food web, "predators" as benthic predators, and "seabird" and "benthic fish" as top predators. We analyze whether trophic level and feeding strategy influence megabenthos iHg, MeHg, and/or tHg content. The observations are analyzed by visualizing the data, performing a linear regression, and plotting a correlation matrix of the difference in bioaccumulation between different feeding strategies. The total and partial R^2 of the linear regression of the effect of the feeding strategy, the trophic level, and the feeding strategy are compared to analyze the effect of both drivers on bioaccumulated iHg, MeHg and tHg.

https://doi.org/10.5194/egusphere-2025-1494
Preprint. Discussion started: 24 April 2025

2.2 The models

To further assess the importance of the feeding strategy, we modeled bioaccumulation in megabenthos, with the feeding strategy being the only distinction between different groups of megabenthos. Then we compared our model to observations to evaluate whether this approach allows us to accurately model bioaccumulation or if additional drivers should be taken into account. We used a fully coupled 1D water column model that is run in 2 setups that resemble typical hydrological regimes found in coastal oceans. We coupled the Generalized Ocean Turbulence Model (GOTM) with the ECOSMO E2E ecosystem model and the Mercy v2.0 Hg speciation and bioaccumulation model.

2.3 The hydrodynamical model

The hydrodynamics of the model are estimated using the GOTM, which is a 1D hydrodynamic model (Bolding et al., 2021). GOTM calculates the turbulence of a vertical 1D water column set-up by computing the solutions to the one-dimensional version of the transport equation of momentum, salinity, and temperature. The model is nudged to observational data sets for temperature and salinity. The setups are based on gridded bathymetry data for water depth with 1/240° resolution (GEBCO Bathymetric Compilation Group, 2020), ECMWF ERA5 dataset for meteorological data (Wouters et al., 2021), Ocean Atlas for salinity and temperature profiles (Garcia H.E. et al., 2019), and the TPOX-9 atlas for tides (Egbert and Erofeeva, 2002), which is combined using the iGOTM tool (https://igotm.bolding-bruggeman.com). The GOTM model is coupled using the Framework for Aquatic Biogeochemical Modeling (FABM) (Bruggeman and Bolding, 2014). The biogeochemical models are encoded in FABM. The FABM interfaces communicate the state variables between the GOTM model and the biogeochemical models.

2.4 The Mercy v2.0 model

Hg cycling and speciation is modeled using the Mercy v2.0 model (Bieser et al., 2023). The Mercy v2.0 model is a comprehensive Hg cycling model that includes speciation between 7 forms of Hg and partitioning to both dissolved organic matter (DOM) and detritus. It was originally developed as a 3D Hg cycling model of the North and Baltic Seas. However, in this study, we use the 1D version of this model, which is driven using the GOTM model. This configuration is used, described, and evaluated in more detail in (Amptmeijer et al., 2025).

2.5 ECOSMO E2E

The ecosystem model is based on the ECOSMO E2E (ECOSystem Model End-to-End) ecosystem model (Daewel et al., 2019). This model extends the ECOSMO II model to have higher trophic levels while preserving consistency at lower trophic levels (Daewel et al., 2019). The version used in this study is the same as the version used and evaluated in (Amptmeijer et al., 2025). In this version, small modifications have been made, such as lowering the mortality rate of zooplankton and decreasing the efficiency of carbon uptake to make the model more suitable for bioaccumulation compared to the version published by (Daewel et al., 2019). The model is evaluated and shown to reproduce the bioaccumulation of iHg and MeHg at the base of the food

https://doi.org/10.5194/egusphere-2025-1494
Preprint. Discussion started: 24 April 2025

web within 1 standard deviation of observations for phytoplankton, microzooplankton, and mesozooplankton. Furthermore, the model accurately models the bioconcentration of both iHg and MeHg and the biomagnification of MeHg within the range of observations.

2.6 Model development

To use the model to study bioaccumulation in megabenthos, the higher trophic level of the ECOSMO E2E model is altered. We exchanged the functional group macrobenthos, fish 1, and fish 2 with 5 megabenthos functional groups, as shown in Fig. 1. The megabenthos groups are separated by their feeding strategy: filter feeder, deposit feeder, generalist feeder, suspension feeder, predator, and top predator.

Filter feeders filter suspended particles from the water column. In our model, they can eat phytoplankton, zooplankton, and detritus. Examples of filter feeders are mussels, tubeworms, and barnacles. The second group is **deposit feeders**. These animals consume organic carbon from the sediment; in our model, they exclusively feed on organic carbon deposited in the sediment. This group would include gastropods and polychaete worms, such as the lugworm (*Arenicula marina*). The **generalist feeder** resembles animals such as North Sea shrimp (*Crangon crangon*), which can utilize various feeding strategies. In our model, this group feeds on phytoplankton, zooplankton, detritus, and deposited material. We also include a **suspension feeder**. Suspension feeders, such as sponges, can consume detritus and DOM. The consumption of DOM, which is too small to be consumed by filter feeders, differentiates suspension and filter feeders. A common strategy to consume DOM as a food source is the utilization of symbiotic bacteria such as chemosymbiotic bivalves from the families Lucinidae, Solemyidae, and Thyasiridae and microbial biomes of high microbial assemblage sponges (Dufour, 2018; Olinger et al., 2021). Finally, we included 2 predators. The first predator is referred to as **the predator**, it feeds on the 4 benthic groups mentioned above, and it has an equal preference and grazing rate in all groups, but it will prioritize abundant groups. This preference is caused by making the food available for predation by the predators not linearly related to the abundance of the prey, but calculated as:

$$b_{\text{available}} = \begin{cases} b_{\text{biomass}}, & \text{if } b_{\text{biomass}} \geq b_{\text{protected}}, \\ b_{\text{biomass}} \frac{b_{\text{biomass}}}{b_{\text{protected}}}, & \text{if } b_{\text{biomass}} < b_{\text{protected}}. \end{cases}$$

in which,

- $b_{\text{available}}$: Portion of prey biomass in g C m^{-2} accessible to predators.
- $b_{\text{protected}}$: Level of prey biomass in g C m^{-2} below which hunting becomes less optimal or energetically inefficient.
- b_{biomass}: Total prey biomass in g C m^{-2} in the environment.

$b_{\text{protected}}$ is 1 g C m^2 for all megabenthos groups, and 0.5 g C m^2 for the benthic predator. This relationship models 2 real-world interactions. First, when the concentration of prey is low, the small number of individuals can more likely survive under ideal circumstances and, therefore, may be less exposed to predation (Campanella Id et al., 2019). Secondly, several predators, such as the shore crab, adapt their behaviors to the density of the prey and learn to be more efficient in the hunting of more common prey (Chakravarti and Cotton, 2014).

https://doi.org/10.5194/egusphere-2025-1494
Preprint. Discussion started: 24 April 2025

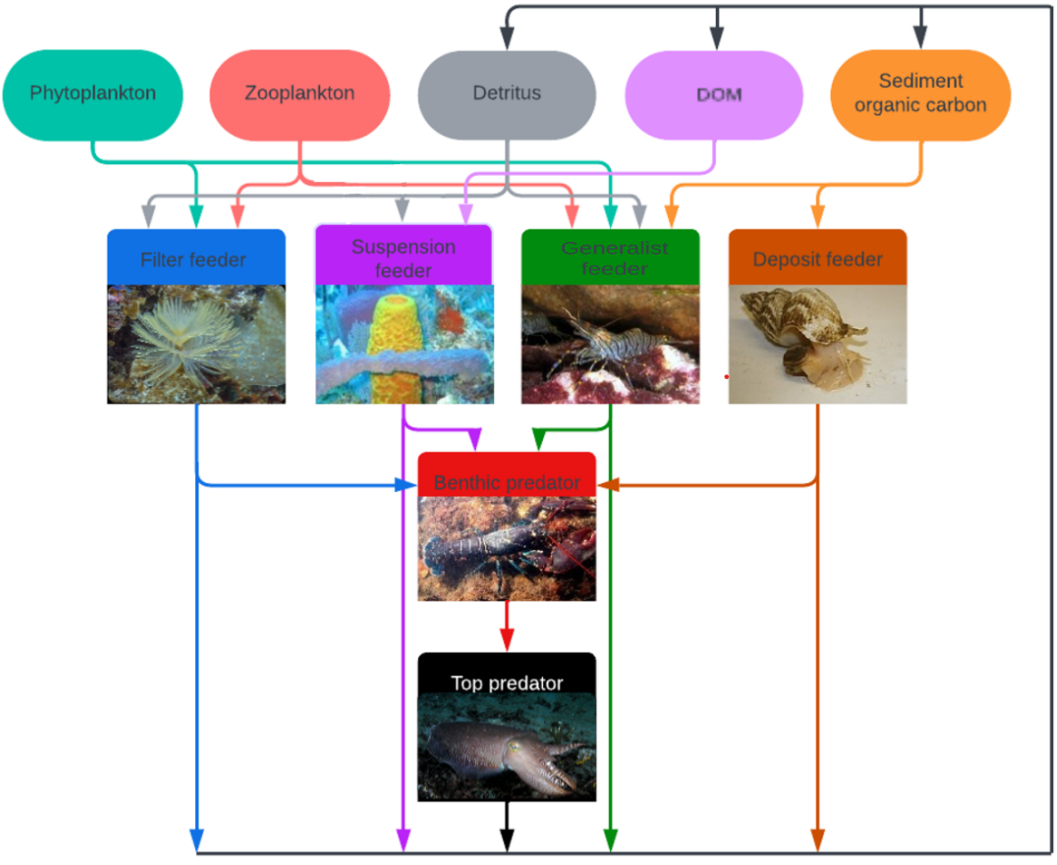

Figure 1. The overview of the modeled megabenthos functional groups and how they interact with each other and functional groups in the ECOSMO E2E model. There are 5 macrobenthic functional groups. The filter feeder feeds on pelagic detritus, zooplankton, and phytoplankton. The suspension feeders feeds on pelagic detritus, phytoplankton, zooplankton, and DOM. The generalist feeds on phytoplankton, zooplankton, pelagic detritus, and sediment organic carbon. The deposit feeder feeds on sediment organic carbon. The benthic predator feeds on the other 4 megabenthos functional groups and the top predator solely feeds on the benthic predator. Several sub-images have been used in this image. Sources of the images are: filter feeder: https://en.wikipedia.org/wiki/Sabella_spallanzanii, suspension feeder: https://www.flickr.com/photos/noaaphotolib/5015046804/, generalist feeder: https://en.wikipedia.org/wiki/Shrimp, deposit feeder: https://nl.wikipedia.org/wiki/Buccinum_undatum, benthic predator: https://en.wikipedia.org/wiki/Lobster, and top predator: https://en.wikipedia.org/wiki/Cuttlefish.

2.7 Assimilation efficiency of iHg and MeHg

The assimilation efficiency (AE) of iHg and MeHg is a key parameter in correct biomagnification modeling. AE is based on laboratory experiments that analyze AE in phytoplankton (Metian et al., 2020; Wang and Wong, 2003). An assimilation

https://doi.org/10.5194/egusphere-2025-1494
Preprint. Discussion started: 24 April 2025

efficiency of 0.95 for MeHg and 0.31 for iHg is chosen for everything except deposit feeding, which has a lower feeding efficiency of 0.07 for iHg and 0.43 for MeHg according to Dutton and Fisher (2012).

2.8 Semi-labile DOM

In the ECOSMO E2E model, only labile-DOM is resolved. This means that there is very little DOM. In our model, we want to incorporate a suspension feeder that would utilize DOM as a food source. Because of this, we added a DOM component referred to as semi-labile DOM. This semi-labile DOM has the same bacterial degradation rate as that of the detritus, and it has the same Hg partitioning behavior as labile DOM. 5% of the organic carbon (Detritus+labile-DOM+semi-labile-DOM) formed, is formed as semi-labile DOM, and there is a breakdown of the detritus into semi-labile DOM of 0.001 d^{-1}. Since the categorization of DOM is very complex, these rates are estimated to create a low maximum of 50 mg C m^{-3}. This is lower than the DOM concentrations typically found in the North Sea, but because it is unclear which fraction of DOM can be consumed by suspension feeders, this amount provides suspension feeders a unique food source that they can utilize while not outcompeting other megabenthos (Lønborg et al., 2024).

2.9 Allometric scaling model

Finally, we run the model while taking into account other drivers of MeHg bioaccumulation to see whether it improves the model. There are three interactions that we take into account for this second model. First, the allometric scaling law, which states that larger animals have a lower base metabolic rate when normalized to body weight (da Silva et al., 2006). Secondly, we account for the observations that MeHg bioaccumulation in fish increases as the water temperature increases, indicating that increased activity does not increase MeHg excretion while it increases MeHg uptake due to a higher grazing rate (Dijkstra et al., 2013). Finally, we assume that predators need to spend more energy on active metabolism to hunt their prey. Because of this, we assumed that the total relative respiration rate of predators and top predators is not altered, so both models have the same carbon cycle. However, MeHg is excreted at a lower rate of 0.002 d^{-1}, rather than their respiration rate, which is the same base metabolic rate as the fish in the ECOSMO E2E model. This leads to a higher bioaccumulation of MeHg at higher trophic levels. The bioaccumulation of iHg is not altered between the two models. In the evaluation, the second model is referred to as the allometric scaling (AS) model.

2.10 The physical setups

The model runs in 2 setups, the first is a 41.5 m deep permanently mixed Southern North Sea set of 41.5 m deep and the second is a seasonally mixed 110 m Northern North Sea setup. These setups are described in more detail in Amptmeijer et al. (2025). The Southern North Sea setup is located at ($54°15'00.0"N$ $3°34'12.0"E$). It is a shallow station that is permanently mixed, meaning that megabenthos can feed directly from the phytoplankton and zooplankton bloom. The setup is chosen because it resembles perfect growth conditions for megabenthos, and most megabenthos in the observations are sampled from similar

https://doi.org/10.5194/egusphere-2025-1494
Preprint. Discussion started: 24 April 2025

circumstances. Because of this, samples are sampled from shallow well-mixed coastal areas, and we used this setup to evaluate the performance of the models.

The Northern North Sea setup is located at ($57°42'00.0"N$ $2°42'00.0"E$) and is only mixed in winter. This means that megabenthos cannot feed directly from the bloom, but are rather dependent on the sinking of detritus particles. In nature, these deeper areas typically have lower overall biomass. This setup is used to evaluate whether the models predict a difference in the bioaccumulation of iHg and MeHg under a different hydrodynamic regime.

2.11 Model evaluation

The goal of the model is to evaluate how well we can model the bioaccumulation of iHg and MeHg while only taking into account trophic interactions. To this extent, the model's result is its performance. If the model performs well, we can conclude that only taking into account trophic interactions explains a large amount of the variability in Hg bioaccumulation. Initially we performs this comparison between observations and the modeled Southern North Sea setup. This is done because most samples are collected from shallow areas that are rich in macrobenthos. Our well mixed Southern North Sea setup would resemble the majority of the observations better than the seasonally mixed Northern North Sea. Afterward, the models are compared to the Northern North Sea models and the AS model to evaluate the effect of hydrodynamics and increased bioaccumulation in higher trophic level animals on our conclusions. The feeding strategy "grazer" was omitted, as the ECOSMO E2E model does not include benthic algae to graze on. The modeled generalist was compared to the deposit and filter feeder from the observations and the modeled top predator to the benthic fish and seabird feeding strategies from the observations. We first calculated the normalized bias as $(modeled - observed)/modeled$ for the average modeled and observed values. Then, we performed a Monte Carlo simulation in which we estimated the mean and standard deviation of the observed and yearly mean of the modeled data of the last 10 years of the simulation. Over 100,000 iterations, we estimated the probability that the modeled value is within 2 standard deviations of the observations, so it checks if the modeled mean is not outside 95% of the observations. After this, we quantified the probability that the modeled mean is of the same distribution as the observations by performing a Bayes factor analysis. The Bayes factor value is estimated by first estimating the likelihood of the modeled mean under the H0 hypothesis, which assumes that the modeled and observed data share the same distribution, and the H1 hypothesis, which assumes that they do not share a distribution. The likelihood of the H1 hypotheses over the H0 hypotheses is the BF10 value. The BF10 factor is estimated using a Jeffreys–Zellner–Siow prior assumption so we assume no prior knowledge. Finally, the total model performance is evaluated by calculating the Root Mean Square Error (RMSE), the Normalised Root Mean Square Error (NRMSE), and the R^2 of the model for iHg and MeHg. In general, a normalized bias between <0.5 can be seen as low. The probability that the model values are not within 2 standard deviations is considered bad and indicates that the modeled mean is a considerable outliers compared to the data. A BF10 factor below 1 indicates that the modeled distribution is more likely the same as the observed distribution, and a BF10 <0.1 can be considered strong evidence and a BF10 <0.01 as very strong evidence in favor of the H0 hypotheses. A lower RMSE shows better model predictive capacity and an NRMSE below 0.5 is indicative of a good fit, while the R^2 is a value between 0 and 1, and closer to 1 shows a better fit.

https://doi.org/10.5194/egusphere-2025-1494
Preprint. Discussion started: 24 April 2025

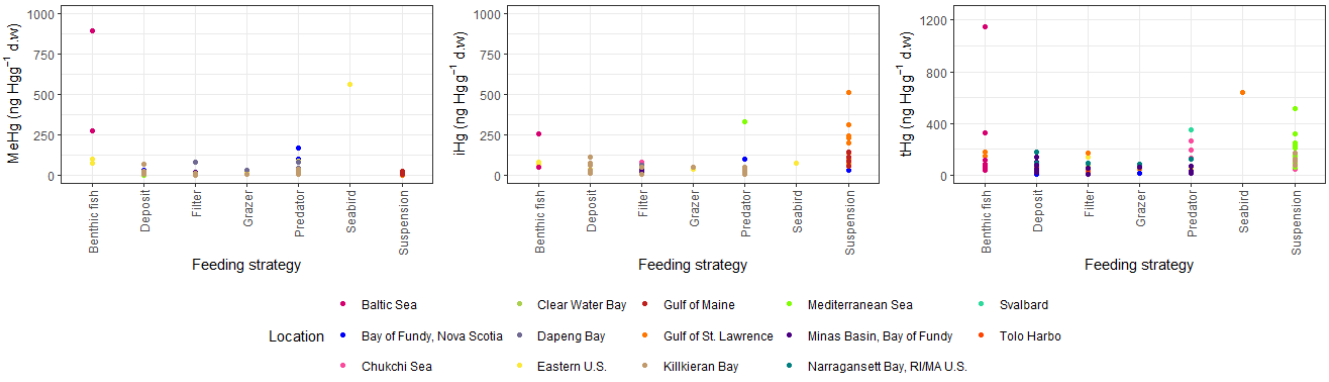

Figure 2. The effect of different feeding strategies on the measured MeHg and iHg in several benthic functional groups and groups of animals feeding on the benthos. The seabird is the common eider which feeds on benthos. Bioaccumulated MeHg is below 50 ng g^{-1} d.w. for all functional groups that are not predatorial (predators, benthic fish, and seabirds), but can reach up to 171, 565, and 895 ng g^{-1} d.w. for predators, seabirds, ad benthic fish respectively. This contrasts the iHg concentration below 100 ng g^{-1} d.w. for every animal. Except for starfish, Eel, and sponges. The tHg shows that the Hg can even be higher in suspension feeders (in this case sponges) than in fish.

3 Results and discussion

3.1 Literature study

The results of our literature study, depicted in Fig. 2, demonstrate that the feeding strategy affects the bioaccumulation of different benthic groups. If we only look at the groups that would represent the base of the benthic food web (filter feeder, suspension feeder, grazer, deposit feeder, and generalist) and perform an ANOVA, we see that there is greater significance of the effect of the feeding strategy ($p = 0.001$) on the bioaccumulation of iHg than on the bioaccumulation of MeHg ($p=0.09$). If we compare the median iHg and MeHg between organisms with different feeding strategies, we see that iHg is lowest in the benthic predator, followed by the deposit feeder, the top predator, the generalist, and the filter feeder, and the highest values are in the suspension feeders. Suspension feeders have by far the highest iHg concentrations and are more than double that of the second highest group, the filter feeders. At the same time, MeHg shows a very different pattern in which suspension feeders have low values, roughly half of that of filter, deposit, and generalist feeders, whereas the predators and top predators are higher.

Figure 3 illustrates the correlation between the bioaccumulation of iHg, MeHg, and tHg. We observe a strong correlation ($R^2=0.49$, $p<0.001$) between MeHg and trophic levels, while no correlation is found between iHg and trophic levels ($R^2<0.02$, $P=0.474$). The linear fit of the intercept of the equations for the iHg and MeHg intercept at trophic level 3.6, which means that below trophic level 3.6 the majority of tHg will on average be iHg.

In Table 1 we show the results of a linear regression taking into account both the trophic level and the feeding strategy, the relative fit of each model explains Hg bioaccumulation based on both factors. The trophic level and feeding strategy are adapted

https://doi.org/10.5194/egusphere-2025-1494
Preprint. Discussion started: 24 April 2025

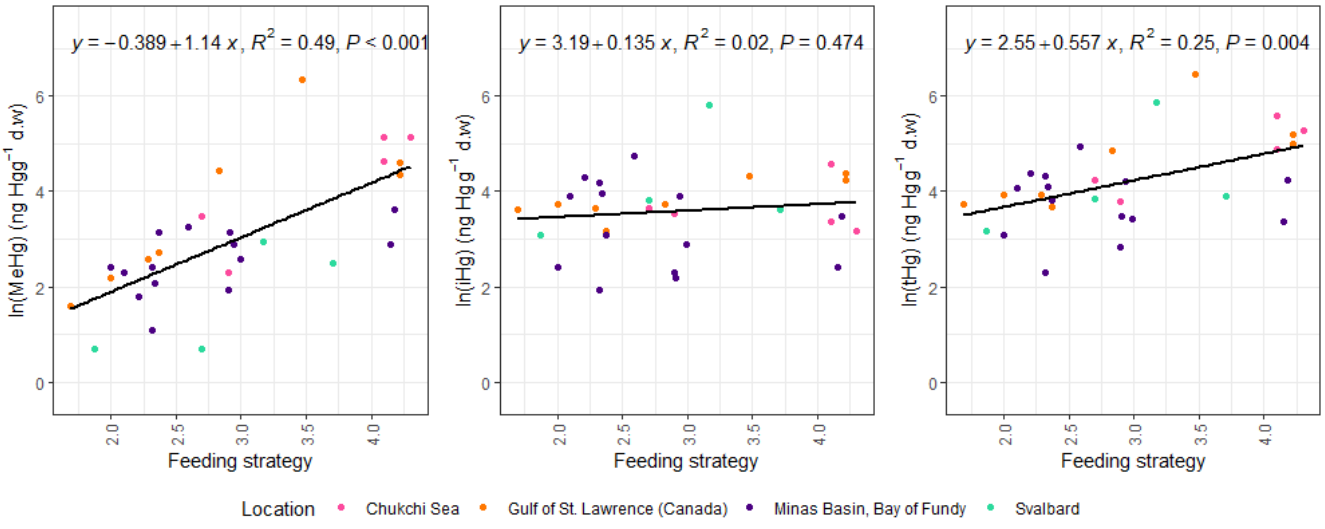

Figure 3. The correlation between the bioaccumulation of MeHg, iHg, and tHg. There is a strong correlation between MeHg and trophic level with a slope of 1.14 ln(ng Hg g^{-1} d.w.) trophic $level^{-1}$ with a R^2 of 0.49, while there is almost no correlation between iHg and trophic level (with a slope of 0.135 ln(ng Hg g^{-1} d.w.) trophic $level^{-1}$ with a R^2 of 0.02. The intercept is, however, much higher for iHg (3.3 at TL=1) than for MeHg (0.8 at TL=1). The tHg combines the 2 patterns with an intercept of 3.1 at TL=1 and a slope of 0.557.

to the natural logarithms of iHg, tHg, and MeHg. This shows that we can explain the bioaccumulation of ln(MeHg) very well (R^2=0.72) with a linear model that takes both drivers into account, while the bioaccumulation of iHg is poorly explained (R^2=0.11) and the bioaccumulation of tHg has an average fit (R^2=0.46). Furthermore, we show the unique contributions of the fit of each driver, the partial R^2. Note that feeding strategy and trophic level can sometimes co-correlate, especially in the case of high MeHg bioaccumulation in predators, benthic fish, and seabirds, as predators are naturally higher in trophic level than the prey they consume. The feeding strategy has an explanatory power larger than that of the trophic level for tHg and iHg, while it is similar for MeHg. Despite the limitations mentioned above, this still shows that the partial R^2 for the feeding strategy is double that of the trophic level, demonstrating the importance of the feeding strategy for the bioaccumulation of tHg at the base of the food web.

Table 1. R-squared and Partial R-squared Results for ln(THg), ln(iHg), and ln(MeHg)

Model	ln(tHg)	ln(iHg)	ln(MeHg)
Full Model R-squared	0.46	0.11	0.72
Partial R-squared (Feeding Strategy)	0.22	0.089	0.32
Partial R-squared (Trophic Level)	0.10	0.012	0.31

https://doi.org/10.5194/egusphere-2025-1494
Preprint. Discussion started: 24 April 2025

In Fig. 4 we show the pairwise comparison of the correlation between the bioaccumulation of iHg, MeHg, and tHg. This shows a clustering in which filter and deposit feeders have similar MeHg concentrations, but MeHg concentrations are lower in grazers and suspension feeders. The strong difference between suspension and filter feeders is especially notable as they both feed on pelagic organic carbon. Overall, this demonstrates that nuanced differences in MeHg bioaccumulation where the concentration in the suspension feeders < grazers < deposit feeders < filter feederss. For iHg the pattern is different; deposit feeders, filter feeders, and grazers have similar iHg, while the iHg content of suspension feeders is much higher.

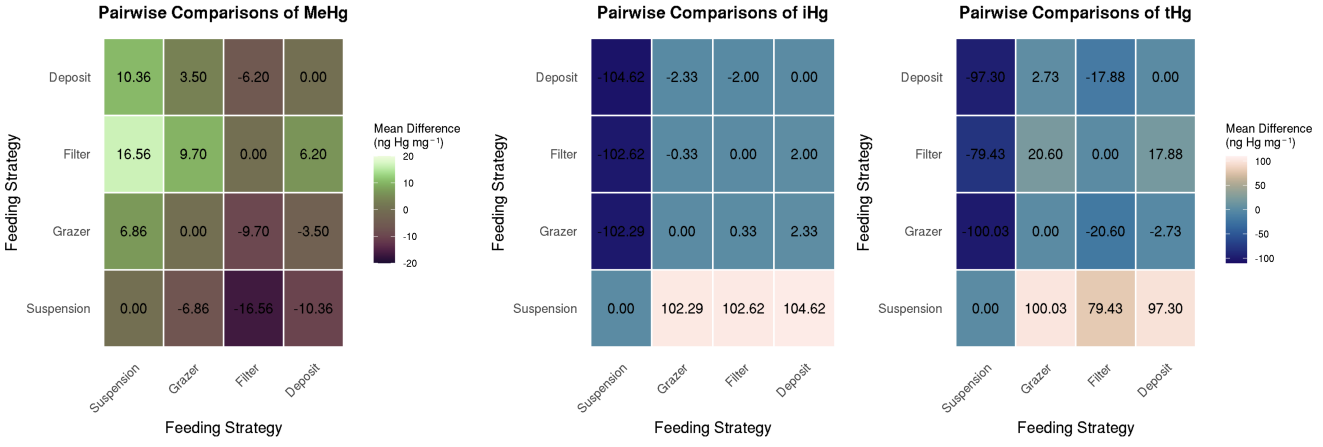

Figure 4. The pairwise comparison of the correlation between the bioaccumulation of MeHg, iHg and tHg and different feeding strategies. For clarity, MeHg has its own scale and iHg and tHg have the same scale. For the concentration of MeHg there is a pattern where suspension feeders < grazers < deposit feeders < filter feeders. For iHg this is different and the main notable difference is much higher iHg in suspension feeders than in any other feeding strategy. tHg is the sum of MeHg and iHg and consequently shows very high tHg in suspension feeders due to the high iHg, and elevated tHg in filter feeders due to their high MeHg.

3.2 Model results

3.2.1 Biomass

Although our megabenthos groups only vary in feeding rate and, therefore, have no direct real-world counterpart to compare to, it is important to validate that they survive in the model. The yearly progression of megabenthos in the Southern North Sea setup is shown in Fig. 5. Filter feeders have the highest biomass, which is up to 10 g C m^{-2} followed by deposit feeders with 5 up to g C m^{-2}, generalist feeders with up to 3 g C m^{-2}, and suspension feeders with up to 1 g C m^{-2}. Higher trophic levels have lower biomass, with up to 0.2 g C m^{-2} for the predator and 0.5 g C m^{-2} for the top predator. This shows that after a simulation period of 20 years, all megabenthos have a stable population, while biomass is highest at the base of the food web.

https://doi.org/10.5194/egusphere-2025-1494
Preprint. Discussion started: 24 April 2025

3.2.2 Bioaccumulation

The modeled bioaccumulation of iHg, MeHg, and tHg is shown in Fig. 6 and the evaluation is shown in Table 3. Note that the values are expressed in ng Hg mg C^{-1}, as this is the best proxy in our model to show the dietary uptake of Hg per energy and nutrients consumed. There is a very high concentration of iHg in the sediment, detritus, and DOM. These values are 0.22, 0.83, and 1.9 ng Hg mg C^{-1} for iHg and 0.038, 0.0046, and 0.0082 ng Hg mg C^{-1} for MeHg. The high amount of iHg in organic carbon is in line with observations that found values of up to 0.114-1.192 ng Hg mg d.w. in sediment in the Scheldt estuary and that DOM strongly binds up to 1.0 ng Hg mg^{-1} (Zaferani and Biester, 2021; Haitzer et al., 2002; Muhaya et al., 1997), which would approximate our modeled 1.9 ng Hg mg C^{-1} if we assume a carbon to weight ratio of 1:2. These high iHg values in DOM lead to high values in suspension feeders in both setups. The bioaccumulation of MeHg is very different from that of iHg and has the highest bioaccumulation in the top predators and predators, followed by deposit feeders and suspension feeders. In Fig. 7 the relationship between the trophic level and the bioaccumulation of iHg and MeHg in megabenthos is shown. There is an increase in the MeHg content with trophic levels that are not present for iHg. For iHg, there is weak anti-correlation (R^2 = 0.20), which is mainly caused by the extremely high iHg content of the low-trophic-level suspension feeders. There is no positive relationship between the bioaccumulation of tHg and the trophic level, while this is present in the allometric scaling model; this indicates that our base model underestimates the bioaccumulation at higher trophic levels.

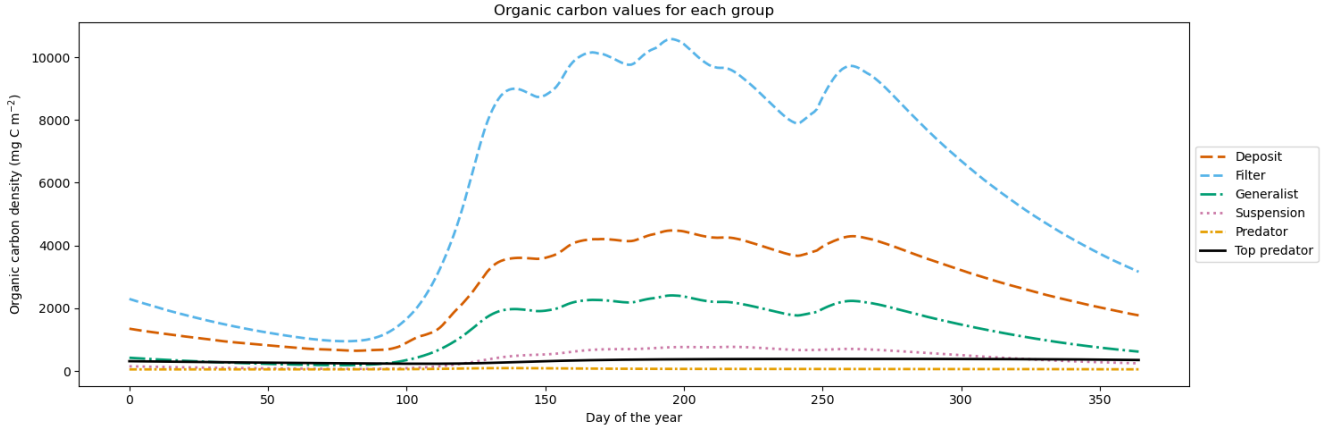

Figure 5. Megabenthos biomass in the modeled Southern North Sea, dominated by filter feeders, followed by deposit feeders, generalist feeders, suspension feeders, predators, and top predators. Biomass fluctuates between 10 and 15 gC m^{-2} and all functional groups have stable populations

3.2.3 The effect of feeding strategy on bioaccumulation

The range and average of the annual average values of the bioaccumulation of iHg and MeHg in our model and the range and mean of measured iHg and MeHg are shown in Table 2. All values fall within the range of observations, except for the

https://doi.org/10.5194/egusphere-2025-1494
Preprint. Discussion started: 24 April 2025

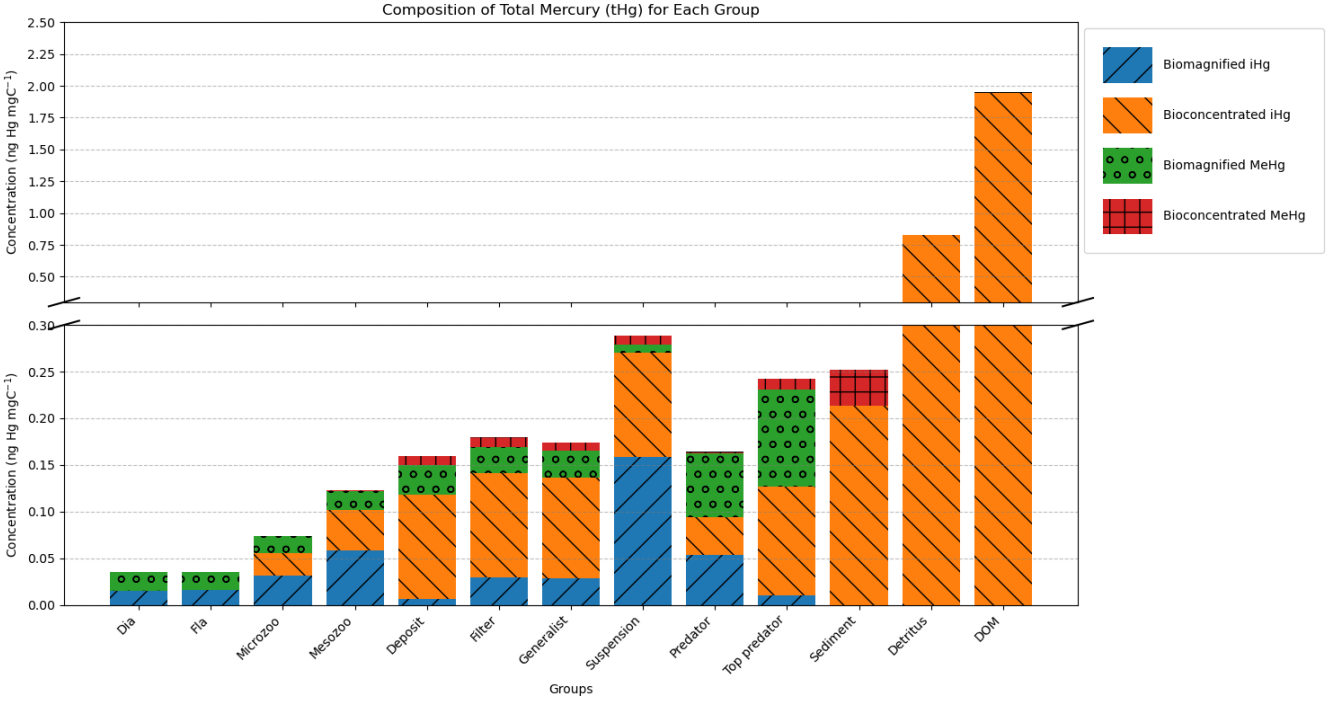

Figure 6. Modeled bioconcentration and biomagnification of iHg and MeHg. Partitioning to detritus and DOM is colored as bioconcentration. The y-axis is cut to show the high and low values. Notably is the high iHg to mgC ratio of detritus and DOM, leading to elevated iHg in suspension feeders. Additionally, higher trophic level animals have higher biomagnified MeHg.

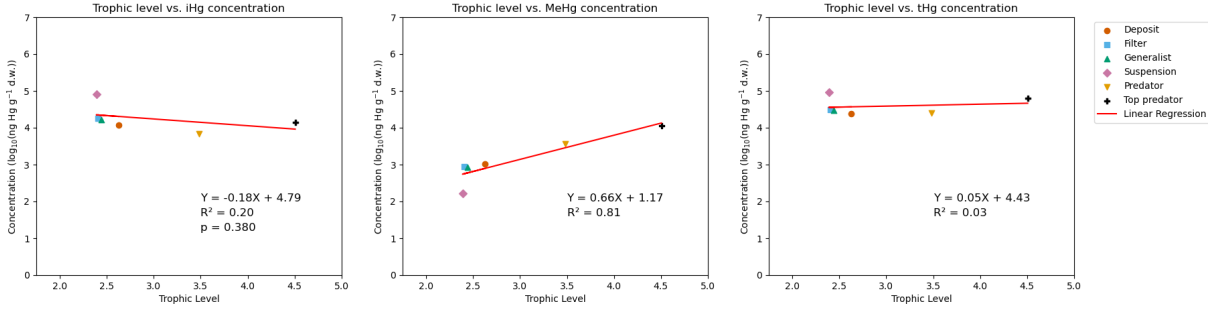

Figure 7. Relationship between the natural logarithm of bioaccumulated MeHg, iHg, and tHg with trophic level. There is a strong relationship between modeled MeHg and trophic level (R^2=0.81) but not for iHg (R^2=0.20) or tHg (R^2=0.03).

https://doi.org/10.5194/egusphere-2025-1494
Preprint. Discussion started: 24 April 2025

modeled top predator in the base model. In the allometric scaling model, the top predator has values for both iHg and MeHg in both the Southern North Sea and the Northern North Sea that are within the range of observations. Although the variation in measured iHg is considerable, suspension feeders consistently have high iHg values. MeHg is bioaccumulated more efficiently and has a higher assimilation efficiency. Because of this, MeHg content is not as dependent on the feeding strategy but is mostly dependent on the trophic level. The mean MeHg is lowest in suspension feeders (9 ng Hg g^{-1} d.w.) while it is very similar for deposit feeders (22 Hg g^{-1} d.w.), filter feeder (19 Hg g^{-1} d.w.) and generalist feeders (19 Hg g^{-1} d.w.). It is notably higher for predators and highest for top predators with a median value of 36 and 59 ng Hg g^{-1} d.w. respectively.

3.2.4 Trophic level vs bioaccumulation

The relationship between the trophic level and the bioaccumulation of iHg, MeHg, and tHg for the literature study is shown in Fig. 3, and for the model is shown in Fig. 7. In both the literature study and our model, there is no strong correlation between trophic level and iHg bioaccumulation. In the literature study, $R^2 < 0.01$ and in our model there is an anti-correlation of $R^2 = 0.20$. In both cases, there is a strong correlation between the bioaccumulation of MeHg and the trophic level. This is $R^2 = 0.49$ for the literature study and $R^2 = 0.81$ in our model. Our model does have a lower effect on the trophic level on MeHg bioaccumulation. Figure 8 shows the relationship between the trophic level and bioaccumulation in the allometric scaling model. There is a notable increase in the correlation between the bioaccumulation of MeHg and tHg with the trophic level compared to the base model.

Table 2. Comparison of modeled and observed Hg and MeHg bioaccumulation in different feeding strategies for the Southern North Sea (SNS), Northern North Sea (NNS), and field observations. Values are presented as ranges with means in parentheses. Units are ng Hg g d.w. for iHg and MeHg, and % for MeHg percentage.

	Model (SNS)			Model (NNS)			Observations		
	iHg	**MeHg**	**% MeHg**	**iHg**	**MeHg**	**% MeHg**	**iHg**	**MeHg**	**% MeHg**
Suspension	104-155 (130)	8-11 (9)	7	60-148 (100)	5-11 (7)	7	34-515 (146)	1-26 (8)	5
Filter	63-77 (70)	16-21 (19)	20	66-96(77)	8-11 (9)	9	8-82 (44)	2-83 (25)	36
Deposit	53-66 (59)	19-26 (22)	16	34-56 (44)	8-12 (10)	13	12-113 (42)	2-70 (19)	31
Generalist	61-74 (68)	16-21 (19)	28	58-92(73)	7-11 (9)	9	8-113 (43)	2-83 (21)	33
Predator	45-49 (47)	35-37 (36)	39	38-42 (40)	15-17 (16)	25	1-329 (54)	7-171 (57)	51
Top predator	62-66 (64)	56-61 (59)	46	43-57 (50)	23-32 (27)	31	40-255 (47)	77-640 (158)	84
Predator (AS)	45-48 (47)	41-44 (42)	38	38-42 (40)	17-19 (18)	24	1-329 (54)	7-171 (57)	51
Top predator (AS)	62-66 (64)	249-264 (258)	80	43-57 (50)	101-131 (115)	39	40-255 (47)	77-640 (578)	84

3.3 The allometric scaling law in high trophic level animals

In Table 3 we show that if we take the allometric scaling law into account the model results for high-trophic level animals increase considerably. In Fig. 8 we show the relation between the natural logarithm of bioaccumulation and the trophic level of the allometric scaling model in the Southern North Sea setup. This increases the linear fit to 1.24x-0.26, which has a slope very

https://doi.org/10.5194/egusphere-2025-1494
Preprint. Discussion started: 24 April 2025

Table 3. Statistical analysis of model performance for iHg and MeHg levels by feeding strategy for Southern North Sea (SNS) and Northern North Sea (NNS).

	SNS				NNS			
	iHg		MeHg		iHg		MeHg	
	N. Bias	BF10	N. Bias	BF10	N. Bias	BF10	N. Bias	BF10
Suspension	-0.11	0.11	0.16	0.0070	-0.37	0.12	-0.10	0.070
Filter	0.61	0.045	-0.25	0.031	0.77	0.069	-0.64	0.035
Deposit	0.43	0.035	0.18	0.019	0.052	0.029	-0.47	0.021
Generalist	0.60	0.042	-0.13	0.024	0.71	0.051	-0.60	0.028
Predator	-0.13	0.087	-0.37	0.061	-0.26	0.087	-0.71	0.074
Top predator	-0.44	0.10	-0.84	0.53	-0.56	0.11	-0.93	0.59
Predator (AS)	-0.13	0.087	-0.26	0.059	-0.26	0.087	-0.68	0.071
Top predator (AS)	-0.44	0.10	-0.32	0.37	-0.56	0.11	-0.70	0.47
Overall Model Performance								
RMSE	19		132		27		145	
NRMSE	0.19		0.35		0.26		0.39	
R-squared	0.84		0.86		**0.49**		0.91	
RMSE (AS)	19		51		27		110	
NRMSE (AS)	0.19		0.13		0.26		0.30	
R-squared (AS)	0.84		>0.99		**0.49**		>0.99	

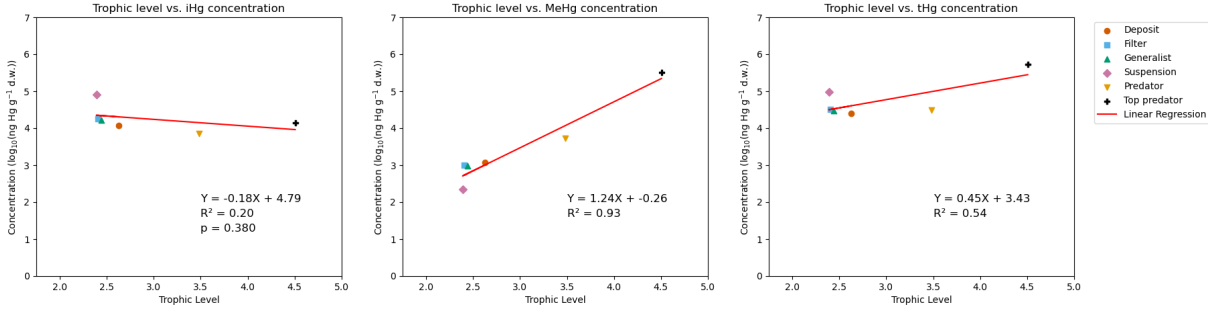

Figure 8. The natural logarithm of the modeled bioaccumulation of iHg, MeHg and tHg in the permanently mixed Southern North Sea using the allometric scaling model is shown against the trophic level. Notably is the stronger slope (1.24) in bioaccumulation of MeHg, which is notably higher than the slope in the default setup (0.66). The slope in the allometric scaling model overlaps much better with the observed relationship of 1.14.

https://doi.org/10.5194/egusphere-2025-1494
Preprint. Discussion started: 24 April 2025

similar to the observed 1.14x + 0.389. Additionally, the normalized bias in the predator and top predators decreased from -0.37 and -0.82 to -0.26 and -0.24, respectively. This is an improvement in the model and shows that while the feeding strategy is an essential driver of Hg bioaccumulation, other differences between high- and low-trophic-level animals should also be taken into account when modeling MeHg bioaccumulation.

3.4 The effect of water column mixing

Finally, if we compare our 2 setups, we find that our model predicts MeHg bioaccumulation three times higher in the shallow permanently mixed Southern North Sea setup than in the deeper seasonally mixed Northern North Sea setup. In our model, this is mostly caused because the megabenthos in the shallow Southern North Sea can feed directly from the phyto-and zooplankton bloom. This gives them greater access to protein-rich food that strongly binds to MeHg. In the Northern North Sea, the ecosystem revolves around the sinking of detritus. Since detritus binds less MeHg than living material, there is a reduction in overall Hg bioaccumulation in the Northern North Sea compared to the Southern North Sea, but especially for MeHg. This means two things. First of all, in the well-mixed Southern North Sea, filter feeders have a competitive advantage as they can filter out fresh food and feed on relatively high trophic level zooplankton. Filter feeders have the highest MeHg values at the base of the benthic food web, and therefore a higher concentration of filter feeders will lead to a higher fraction of filter feeders in the predator diet and thus more MeHg. Additionally, since the filter feeders feed on living pelagic material with higher MeHg values, the filter feeders themselves also have higher MeHg. Thus, predators and, consequently, the top predators have higher MeHg values in the Southern North Sea compared to the Northern North Sea as a result of the increased water column mixing. In Fig. 9 we show the correlation between the natural logarithm of bioaccumulated Hg and the trophic level in the Northern North Sea. Interestingly, the trophic level of megabenthos is higher in the Northern North Sea, while the bioaccumulation level is lower. This is because the detritus is cycled more often in the pelagic before it is consumed by megabenthos, because the detritus is in constant equilibrium with the water column for its partitioning of Hg and MeHg, this does not translate to higher bioaccumulation. This lower bioaccumulation results in lower concentrations of MeHg in high trophic levels of fish.

4 Comparing model and observations

First, we compare the values for iHg. The probability that the model is within 2 standard deviations of the observation is >0.95 in all cases. In most cases, the BF10 factor is < 0.1, which provides strong evidence in favor of the null hypotheses, indicating that the distribution of the model output closely matches the distribution of the observations and suggests that the model accurately reproduces the properties of the observations. The only instance where the BF10 factor >0.1 for iHg is for suspension feeders. This comparison yields several interesting results. Our model estimates that suspension feeders have the highest iHg values, but comparing our model with field observations shows that the observed values are even higher. In our model, the high iHg values are caused by the very efficient Hg scavenging of small DOM particles. These small particles have the highest Hg/C ratio (as was shown in Fig. 6) and can only be consumed by suspension feeders. This leads to very high iHg and low MeHg in suspension feeders. The result that our model partially replicates the high iHg values in the suspension feeders

https://doi.org/10.5194/egusphere-2025-1494
Preprint. Discussion started: 24 April 2025

indicates that we underestimated this effect or that additional factors were contributing to the high iHg levels found. In Orani et al. (2020), it is demonstrated that the extremely low MeHg/Hg ratio in suspension-feeding sponges may be caused by the demethylation of MeHg by symbiotic bacteria. Our study expands on this by showing that the high iHg and low MeHg values can partially be explained by the consumption of DOM by suspension feeders, but the proposed demethylation could explain why we cannot fully replicate the observations. Based on this, it is likely that the unique bioaccumulation values in suspension feeders are caused by a combination of their ability to feed on DOM, together with biochemical processes that occur in their symbiotic bacteria. Notably, while not statistically significant, our model overestimates the mean iHg values with a normalized bias of 0.61 and 0.77 for filter feeders and 0.60 and 0.60 for generalist feeders in the Southern North Sea and Northern North Sea, respectively. In Fig 6 we see that the majority of this iHg originates from bioconcentration. This discrepancy is described in more detail later in the paper.

Our base model fails to reproduce the high values in the top predators, but this is improved in the allometric scaling model. The normalized bias is reduced from -0.84 to -0.32, but the BF10 factor is reduced only from 0.53 to 0.37. This shows that while the modeled mean is closer to the observed mean, there is no strong indication that the modeled values are from the same distribution as the observations. In the allometric scaling model, we get a linear relationship of 1.24x-0.26 (R^2=0.93), which is very similar to the 1.14x+0.389 found in the field observations. The drastic improvement in the allometric scaling model compared to the base model indicates that the lower MeHg release rates in high-trophic-level animals should be taken into account. We tried to run the model with the lower MeHg release rate in all megabenthos, but this resulted in unrealistically high values in both the base and top of the food web, so we cannot just use the lower MeHg release rate at every trophic level. Because of this, we conclude that the difference in the release rate of MeHg-related body size, metabolic rate, or activity likely has a significant contribution to the high MeHg values in high-trophic-level animals.

The last difference between our model and observations is that our model deposit feeders have considerably higher MeHg bioaccumulation compared to generalist feeders, filter feeders, and suspension feeders. This is not the case in the field observations where deposit feeders are similar to filter feeders and generalist feeders in MeHg. Interestingly, we already gave deposit feeders a lower assimilation efficiency compared to other functional groups. Since we do not model actual organisms, this difference can be caused by other differences in the organisms, such as their metabolic rate, or the assimilation efficiency of deposit feeders should be even lower. A final option is that the Mercy v2.0 model is mainly focused and verified on pelagic Hg cycling, so we potentially overestimate the sediment MeHg content or the AE of sediment-bound MeHg.

5 Bioconcentration of iHg

The largest bias in our model, which remains uncorrected in the allometric scaling model, is the overestimation of iHg in the filter, deposit, and generalist feeders. Although the modeled iHg values are not out of the observed range, the consistently high normalized bias indicates that the model overestimates the bioaccummulation of iHg. In Fig. 6 we can see that the vast majority of iHg in filter, deposit, and generalist feeders originates from bioconcentration. The most important driver of bioconcentration is the ratio between uptake and release rate, or the uptake-release ratio. Our model has an uptake-release ratio of 210 l g^{-1}

https://doi.org/10.5194/egusphere-2025-1494
Preprint. Discussion started: 24 April 2025

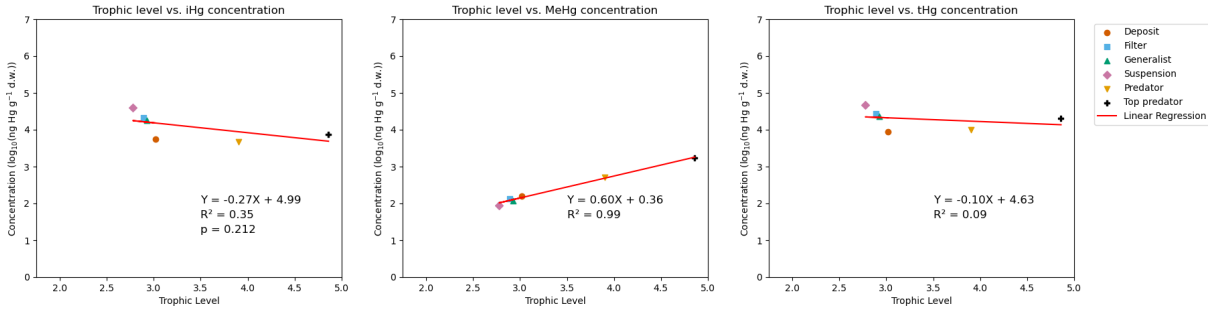

Figure 9. The natural logarithm of the modeled bioaccumulation of iHg and MeHg in the permanently mixed Northern North Sea setup. While the slope is somewhat similar (0.60 vs 0.66) the overall bioaccumulation of MeHg is notably lower than in the permanently mixed Southern North Sea.

d.w. This is derived from Tsui and Wang (2004), as it represents the lowest ratio found in the literature. The exact rate was obtained by withdrawing the modeled carbon excretion rate and deducting this from the measured iHg release rate to have an iHg specific release rate, this rate was found to be 0.04 d^{-1}, as presented in Amptmeijer et al. (2025). Other studies such as Pan and Wang (2011) found higher uptake-release ratios between 424 and 781 l g^{-1} d.w.

To address this uncertainty, we tested an alternative scenario in which we doubled the bioconcentrated iHg release rate, 0.04 d^{-1} to 0.08 d^{-1}, thus lowering the uptake-release ratio to 105 l g^{-1} dw. This adjustment resulted in a normalized bias in the Southern North Sea of -0.09, 0.15 and 0.15 for the deposit, filter, and generalist feeders, respectively. This shows how the uptake and release rates of iHg can impact the iHg content of megabenthos, and that the uptake-release ratio used in the model is likely overestimated.

The discrepancy between the modeled and observed iHg can be caused by several factors. First, iHg concentrations in North Sea megabenthos could be higher than those reported in other coastal zones. However, there are no empirical data to support or invalidate this conclusion at the moment. Secondly, translating experimentally obtained uptake and release rates to observations of iHg might depend on the drivers that are not captured in the model. In either case, it is hard to verify the root of this high normalized bias, as the bioaccumulation of iHg is comparatively understudied compared to the bioaccumulation of MeHg, both in models and empirical studies.

6 Model limitations

Our model is designed to have the same rates for all megabenthos groups. This allows us to isolate the effect of the feeding strategy, but it should be taken into account that this also means that the model is limited in its ability to predict bioaccumulation of iHg or MeHg in specific animals. Furthermore, when our model is compared to the data in the literature, it should be noted that field studies measuring Hg at the base of the food web are rare. Our model is run in the North Sea, while most of the field observations are from different regions. This is somewhat mitigated by aggregating large amounts of data and comparing it to

https://doi.org/10.5194/egusphere-2025-1494
Preprint. Discussion started: 24 April 2025

our idealized water column scenarios to identify general trends, but it must be noted that comparison can always be improved by having more data to compare it to. The first and most notable limitation is that some field studies that analyzed megabenthos benthos did not differentiate between iHg and MeHg and that most studies did not estimate the trophic level of the animals. This is especially problematic when comparing Hg levels with our model.

The difference in bioaccumulation between the permanently mixed Southern North Sea setup and the seasonally mixed Northern North Sea setup is caused by several assumptions in the model. Notably, instant partitioning between dissolved Hg and Hg associated with detritus. The complication with this is that the partitioning coefficients are based on the $\log(k)^{ow}$ values of Hg, while it has been demonstrated that the binding of Hg to organic material also depends on its sulfate content (Seelen et al., 2023). Since the ECOSMO E2E model is a Redfield ratio-based model, we did not take the freshness of the organic material into account, but this might play a role and should be investigated in further studies.

A final interaction that we did not take into account is *in vivo* Hg speciation. This is not taken into account because at the moment there is too much uncertainty about the role this plays in Hg bioaccumulation. However, the earlier mentioned demethylation in sponges by Orani et al. (2020) and additional studies that demonstrate Hg speciation in cuttlefish by Gente` et al. (2023) and Hg methylating bacteria in copepods by Gorokhova et al. (2020) indicate that the bioaccumulation of iHg and MeHg may not be fully independent processes. These could be important interactions, and especially *in vivo*, methylation could be a driver of high MeHg values, but more empirical studies must be performed on the rates of this before this can be incorporated in models in a meaningful way.

7 Summary and conclusion

In this study, we analyze the role of the trophic level and the feeding strategy on the bioaccumulation of iHg and MeHg. We did this by performing a literature study and running a fully coupled 1D model in two idealized setups representing two different hydrodynamics regimes in which macrobenthic communities can live. Our study estimates that the trophic level predicts up to 32% of the variability MeHg in the benthic food web. If we include both the feeding strategy and the trophic level, this increases to 72%. We show that several feeding strategies have significant differences.

We show that there are notable differences between feeding strategies. iHg is higher in suspension feeders and MeHg is low in suspension feeders and grazers, while filter feeders have the highest MeHg followed by deposit feeders. Our model expands on this by demonstrating that we can accurately model the bioaccumulation of iHg and MeHg at the base of the food web by only taking the feeding strategy into account.

Because our base model agrees well with both observed iHg (R^2=0.86) and MeHg (R^2=0.91) in the Southern North Sea setup, we conclude that you can accurately model the bioaccumulation of both iHg and MeHg at the base of the food web based on the feeding strategy. However, this strong performance is mostly because 4 out of our 6 megabenthos groups are low trophic level non-predators, and our base model starts to underperform considerably in its ability to model MeHg bioaccumulation in higher trophic levels. This problem is solved by taking into account the allometric scaling law and assuming that MeHg removal from the organism is not linked to the total but rather to the base metabolic rate. Because of this, we accept our hypothesis that

https://doi.org/10.5194/egusphere-2025-1494
Preprint. Discussion started: 24 April 2025

the feeding strategy is an essential driver of the bioaccumulation of iHg and MeHg in low-trophic-level animals, but other differences in the organisms between high- and low-trophic-level animals should also be taken into account when predicting MeHg values in high-trophic-level fish. Our model and observation focus on lower-trophic-level benthic invertebrates, with some high-trophic-level animals added to create context. The importance of this for the bioaccumulation of MeHg in animals of high trophic levels is that all biomagnification is an exponential function starting at the base of the food web. Therefore, a change in MeHg at the base of the food web will correspond to a similar relative increase at the top of the food chain. Because the feeding strategy has such a large impact on the base of the food web, high trophic-level animals would have considerably different MeHg values depending on the species composition of the base of the food web.

Interestingly, despite the lower biomagnification potential of iHg, its high abundance in certain low-trophic-level animals can lead to higher tHg in low trophic level animals than in higher-trophic-level animals. This discrepancy can distort risk perception, as safety assessments often rely on tHg measurements that do not distinguish between iHg and MeHg. Such animals may have high Hg values while remaining safe for human consumption. Our findings demonstrate the importance of Hg speciation data in marine organisms to help improve food safety guidelines and inform regulatory policies.

7.1 Societal relevance & future work

Our study highlights the critical role of benthic diversity in driving MeHg bioaccumulation. Both trophic interactions and the feeding strategy significantly influence MeHg bioaccumulation, which has important implications for seafood safety and fisheries management. Understanding these processes can help explain the spatial and temporal variability in the MeHg content of fish, which is crucial for policymakers to develop effective regulations that safeguard human health and marine ecosystems.

Our findings suggest that fish from food webs dominated by filter feeders would have the highest MeHg content, since filter feeders have the highest MeHg content in both our model and observations. It also creates an indication that the introduction of bivalve communities in the form of mussel or oyster farming could increase MeHg levels in higher food chains. However, such changes in the ecosystem would inevitably change other factors in the ecosystem, including biomass and trophic interactions that are also essential drivers for MeHg bioaccumulation. This means that case-by-case studies are needed to fully understand how changes in the base of the food web will affect the concentration of MeHg in high trophic level fish.

We strongly recommend targeted field studies that systematically measure iHg, MeHg, and trophic levels in diverse marine communities to assess how the structure of the food web influences the bioaccumulation of MeHg in seafood.

8 Acknowledgments

Readability suggestions for this paper were generated using rAI tools such as ChatGPT (OpenAI), while AI-based spell checks such as Grammarly and Writefull were used to correct spelling. In addition, AI tools helped optimize the R and Python scripts and provide coding suggestions. All suggestions were implemented only after critical manual evaluation. Finally, Google Scholar and Perplexity were used to find sources for literature research, which were consequently manually read, verified, and cited.

https://doi.org/10.5194/egusphere-2025-1494
Preprint. Discussion started: 24 April 2025

Author contributions

The contributions per author are listed in Table 4.

Table 4. Contributions per Author. Authors are: David Johannes Amptmeijer (DA), Andrea Padilla (AP), Sofia Modesti (SM), Prof. Dr. Corinna Schrum (CS), and Dr. Johannes Bieser (JB).

Contributor role	Role definition	Authors
Conceptualisation	Conceptualized the study	DA, JB, CS
	Developed the research objectives	DA, JB, CS
Methodology	Implementation of the model into FABM	DA
	Compiled the database of megabenthos iHg and MeHg observations	DA, AP
Evaluation	Evaluated the model performance against observations	JB, DA, AP, SM
	Performed statistical tests on the observations	DA, AP, SM
Writing	Writing of the original draft	DA
	Review of the original draft and quality control	AP, SM, JB, DA
Supervision	Supervised the development of the work	CS, JB, DA
Funding acquisition	Acquired funding via the GMOS-Train ITN	JB

Conflict of interest

None of the authors declare any conflict of interest.

Funding

This research has been funded by the European Union's Horizon 2020 research and innovation programme under the Marie Sklodowska-Curie grant agreement no. 860497.

https://doi.org/10.5194/egusphere-2025-1494
Preprint. Discussion started: 24 April 2025

Table 5. Data used for the literature study.

Species	Common name	Trophic level	feeding strategy	THg (ng/g d.w.)	MeHg (ng/g d.w.)	Location	Reference
Stronglyocentrotus droebachiensis	Sea urchin	1,87	Deposit	24	2	Svalbard	Korejwo et al. (2022)
Ophiopholis aculeata	Brittle star	2,70	Filter	47	2	Svalbard	Korejwo et al. (2022)
Baccinum glaciale	Glacial whelk	3,71	Deposit	49	12	Svalbard	Korejwo et al. (2022)
Henricia sp	starfish	3,17	Predator	348	19	Svalbard	Korejwo et al. (2022)
Astarte borealis	Northern Astarte	2,90	Suspension	44	10	Chukchi Sea	Fox et al. (2013)
Ampelisca macrocephala	Amphipod	2,70	Deposit	70	32	Chukchi Sea	Fox et al. (2013)
Chinoecetes opilio	Snow crab	4,10	Predator	131	102	Chukchi Sea	Fox et al. (2013)
Neptunea heros	Northern neptune	4,30	Predator	195	171	Chukchi Sea	Fox et al. (2013)
Buccinum spp	Whelk	4,10	Predator	269	171	Chukchi Sea	Fox et al. (2013)
Gammarellus sp.	Gammarid	2,37	Predator	39	15	Gulf of St. Lawrence	Lavoie et al. (2010)
Littorina littorea	Common periwinkle	2,29	Grazer	51	13	Gulf of St. Lawrence	Lavoie et al. (2010)
Buccinum undatum	Waved whelk	2,83	Predator	127	85	Gulf of St. Lawrence	Lavoie et al. (2010)
Tectura testudinalis	Common tortoise limpet	2,00	Grazer	51	9	Gulf of St. Lawrence	Lavoie et al. (2010)
Strongylocentrotus droebachiensis	Green sea urchin	1,69	Deposit	42	5	Gulf of St. Lawrence	Lavoie et al. (2010)
Hippoglossoides platessoides	American plaice	4,22	Benthic fish	146	77	Gulf of St. Lawrence	Lavoie et al. (2010)
Glyptocephalus cynoglossus	Witch flounder	4,22	Benthic fish	179	100	Gulf of St. Lawrence	Lavoie et al. (2010)
Somateria mollissima	Common eider	3,47	Seabird	640	565	Gulf of St. Lawrence	Lavoie et al. (2010)
Anguilla anguilla	European eel		Benthic fish	1161	895	Baltic Sea	Polak-Juszczak (2018)
Gadus morhua	Atlantic cod		Benthic fish	346	269	Baltic Sea	Polak-Juszczak (2018)
Platichtys flesus	European flounder		Benthic fish	77		Baltic Sea	Polak-Juszczak (2014)
Platichtys flesus	European flounder		Benthic fish	58		Baltic Sea	Polak-Juszczak (2014)
Pleuronectes platessa	European plaice		Benthic fish	51		Baltic Sea	Polak-Juszczak (2014)
Pleuronectes platessa	European plaice		Benthic fish	40		Baltic Sea	Polak-Juszczak (2014)
Scophthalmus maximus	Turbot		Benthic fish	114		Baltic Sea	Polak-Juszczak (2014)
sScophthalmus maximus	Turbot		Benthic fish	85		Baltic Sea	Polak-Juszczak (2014)
Macoma balthica	Baltic macoma		Deposit	53		Baltic Sea	Polak-Juszczak (2014)
Macoma balthica	Baltic macoma		Deposit	25		Baltic Sea	Polak-Juszczak (2014)
Saduria entomon	Isopod		Predator	21		Baltic Sea	Polak-Juszczak (2014)
Saduria entomon	Isopod		Predator	14		Baltic Sea	Polak-Juszczak (2014)
Acanthella acuta	Cactus sponge		Suspension	115	6	Mediterranean Sea	Orani et al. (2020)
Acanthella acuta	Cactus sponge		Suspension	66	7	Mediterranean Sea	Orani et al. (2020)
Acanthella acuta	Cactus sponge		Suspension	107	11	Mediterranean Sea	Orani et al. (2020)
Acanthella acuta	Cactus sponge		Suspension	95	9	Mediterranean Sea	Orani et al. (2020)
Axinella damicornis	Crumpled dustor sponge		Suspension	97	2	Mediterranean Sea	Orani et al. (2020)
Axinella damicornis	Crumpled dustor sponge		Suspension	212	9	Mediterranean Sea	Orani et al. (2020)
Axinella damicornis	Crumpled dustor sponge		Suspension	252	7	Mediterranean Sea	Orani et al. (2020)
Chondrilla nucula	Caribbean chicken-liver sponge		Suspension	149	2	Mediterranean Sea	Orani et al. (2020)
Chondrilla nucula	Caribbean chicken-liver sponge		Suspension	233	1	Mediterranean Sea	Orani et al. (2020)
Chondrilla nucula	Caribbean chicken-liver sponge		Suspension	519	4	Mediterranean Sea	Orani et al. (2020)
Chondrilla nucula	Caribbean chicken-liver sponge		Suspension	317	4	Mediterranean Sea	Orani et al. (2020)
Haliclona fulva	Orange encrusting sponge		Suspension	80	3	Mediterranean Sea	Orani et al. (2020)
Haliclona fulva	Orange encrusting sponge		Suspension	76	2	Mediterranean Sea	Orani et al. (2020)
Haliclona fulva	Orange encrusting sponge		Suspension	107	6	Mediterranean Sea	Orani et al. (2020)
Haliclona fulva	Orange encrusting sponge		Suspension	146	6	Mediterranean Sea	Orani et al. (2020)
Halichondria panicea	Breadcrumb sponge		Suspension	81	23	Killkieran Bay	Orani et al. (2020)
Halichondria panicea	Breadcrumb sponge		Suspension	122	9	Killkieran Bay	Orani et al. (2020)
Hymeniacidon perlevis	Breadcrumb sponge		Suspension	107	20	Killkieran Bay	Orani et al. (2020)
Hymeniacidon perlevis	Breadcrumb sponge		Suspension	170	26	Killkieran Bay	Orani et al. (2020)
Chlamys nobilis	Noble scallop		Filter	60	19	Dapeng Bay	Pan and Wang (2011)
Ruditapes philippinarum	Manilla clam		Filter	47	17	Tolo Harbo	Pan and Wang (2011)
Saccostrea cucullata	Hooded oyster		Filter	70	15	Clear Water Bay	Pan and Wang (2011)
Perna viridis	Green mussel		Filter	30	9	Tolo Harbo	Pan and Wang (2011)
Septifer virgatus	Black mussel		Filter	92	10	Clear Water Bay	Pan and Wang (2011)
Ilyanassa obsoleta	Eastern mudsnail		Deposit	60		Gulf of Maine	Chen et al. (2009)
Amphipod spp.	Amphipod		Deposit	12		Gulf of Maine	Chen et al. (2009)
Mytilidae spp	Mussel		Filter	142	79	Eastern U.S.	Chen et al. (2014)
Carcinus maenas	Green Crab		Predator	57	42	Eastern U.S.	Chen et al. (2014)
Mytilidae spp	Mussel		Filter	173		Gulf of St. Lawrence	Cossa and Tabard (2020)
Maldanidae spp.	Bamboo Worm		Deposit	101	70	Minas Basin, Bay of Fundy	Sizmur et al. (2013)
Corophium volutator	Mud scud		Deposit	43	11	Minas Basin, Bay of Fundy	Sizmur et al. (2013)
Glyceridae spp.	Bloodworm		Predator	37	9	Minas Basin, Bay of Fundy	Sizmur et al. (2013)
Mytilidae spp	Mussel		Filter	95		Narragansett Bay, RI/MA U.S.	Taylor et al. (2012)
Nereidae spp.	Ragworm		Deposit	139		Narragansett Bay, RI/MA U.S.	Taylor et al. (2019)
Amphipod spp.	Amphipod		Deposit	93		Narragansett Bay, RI/MA U.S.	Taylor et al. (2019)
Carcinus maenas	Green Crab		Predator	126		Narragansett Bay, RI/MA U.S.	Taylor et al. (2019)
Carcinus maenas	Green Crab		Predator		80	Eastern U.S.	Taylor et al. (2019)
Mytilidae spp	Mussel		Filter		83	Eastern U.S.	Taylor et al. (2019)
Ilyanassa obsoleta	Eastern mudsnail		Deposit	177		Narragansett Bay, RI/MA U.S.	Taylor et al. (2019)
Litorrina littorea	Common periwinkle		Grazer	90		Narragansett Bay, RI/MA U.S.	Taylor et al. (2019)
Litorrina littorea	Common periwinkle		Grazer		30	Eastern U.S.	Taylor et al. (2019)
Corophium volutator	Mud scud		Deposit	10		Bay of Fundy, Nova Scotia	English et al. (2015)
Macoma balthica	Baltic macoma		Deposit	10		Bay of Fundy, Nova Scotia	English et al. (2015)
Ilyanassa obsoleta	Eastern mudsnail		Deposit	40		Bay of Fundy, Nova Scotia	English et al. (2015)
Litorrina littorea	Common periwinkle		Grazer	20		Bay of Fundy, Nova Scotia	English et al. (2015)
Nereidae spp.	Ragworm		Deposit	10		Bay of Fundy, Nova Scotia	English et al. (2015)
Maldanidae spp.	Bamboo Worm		Deposit	20		Bay of Fundy, Nova Scotia	English et al. (2015)
Balanus balanus	Acorn barnacle	2,32	Filter	10	3	Minas Basin, Bay of Fundy	Bradford et al. (2023)
Carcinus maenas	Green Crab	2,91	Predator	32	23	Minas Basin, Bay of Fundy	Bradford et al. (2023)
Corophium volutator	Mud scud	2,00	Deposit	22	11	Minas Basin, Bay of Fundy	Bradford et al. (2023)
Glyceridae spp.	Bloodworm	4,15	Predator	29	18	Minas Basin, Bay of Fundy	Bradford et al. (2023)
Goniadidae spp.	Goniadidae	4,18	Predator	69	37	Minas Basin, Bay of Fundy	Bradford et al. (2023)
Ilyanassa obsoleta	Eastern mudsnail	2,59	Deposit	139	26	Minas Basin, Bay of Fundy	Bradford et al. (2023)
Lineidae spp.	Ribbon worm	2,99	Deposit	31	13	Minas Basin, Bay of Fundy	Bradford et al. (2023)
Litorrina littorea	Common periwinkle	2,34	Grazer	60	8	Minas Basin, Bay of Fundy	Bradford et al. (2023)
Macoma balthica	Baltic macoma	2,32	Deposit	76	11	Minas Basin, Bay of Fundy	Bradford et al. (2023)
Maldanidae spp.	Bamboo Worm	2,37	Deposit	45	23	Minas Basin, Bay of Fundy	Bradford et al. (2023)
Mytilus edulis	Blue mussel	2,10	Filter	59	10	Minas Basin, Bay of Fundy	Bradford et al. (2023)
Nereidae spp.	Ragworm	2,21	Deposit	80	6	Minas Basin, Bay of Fundy	Bradford et al. (2023)
Pagurus acadiarnus	Acadian hermit crab	2,90	Predator	17	7	Minas Basin, Bay of Fundy	Bradford et al. (2023)
Phyllodocidae spp.	Paddle worm	2,94	Predator	67	18	Minas Basin, Bay of Fundy	Bradford et al. (2023)

https://doi.org/10.5194/egusphere-2025-1494
Preprint. Discussion started: 24 April 2025

References

Amptmeijer, D. J., Bieser, J., Mikheeva, E., Daewel, U., and Schrum, C.: Bioaccumulation as a driver of high MeHg in coastal Seas, In preperation, 2025.

Bieser, J., Amptmeijer, D., Daewel, U., Kuss, J., Soerenson, A. L., and Schrum, C.: The 3D biogeochemical marine mercury cycling model MERCY v2.0; linking atmospheric Hg to methyl mercury in fish, Geoscientific Model Development Discussions, pp. 1–59, https://doi.org/10.5194/GMD-2021-427, 2023.

Bolding, K., Bruggeman, J., Burchard, H., and Umlauf, L.: General Ocean Turbulence Model - GOTM, https://doi.org/10.5281/ZENODO.4896611, 2021.

Bradford, M. A., Mallory, M. L., and O'Driscoll, N. J.: Mercury bioaccumulation and speciation in coastal invertebrates: Implications for trophic magnification in a marine food web, Marine Pollution Bulletin, 188, 114 647, https://doi.org/10.1016/J.MARPOLBUL.2023.114647, 2023.

Bruggeman, J. and Bolding, K.: A general framework for aquatic biogeochemical models, Environmental Modelling & Software, 61, 249–265, https://doi.org/10.1016/J.ENVSOFT.2014.04.002, 2014.

Campanella Id, F., Auster, P. J., Taylor, J. C., and Muñoz, R. C.: Dynamics of predator-prey habitat use and behavioral interactions over diel periods at sub-tropical reefs, PLOS ONE, 2, https://doi.org/10.1371/journal.pone.0211886, 2019.

Chakravarti, L. J. and Cotton, P. A.: The Effects of a Competitor on the Foraging Behaviour of the Shore Crab Carcinus maenas, PLoS ONE, 9, 93 546, https://doi.org/10.1371/journal.pone.0093546, 2014.

Chen, C. Y., Dionne, M., Mayes, B. M., Ward, Darron, M., Sturup Stefan, and Brian, J. P.: Mercury Bioavailability and Bioaccumulation in Estuarine Food Webs in the Gulf of Maine, Environ. Sci. Technol., 43, 1804–1810, https://doi.org/10.1021/es8017122, 2009.

Chen, C. Y., Borsuk, M. E., Bugge, D. M., Hollweg, T., Balcom, P. H., Ward, D. M., Williams, J., and Mason, R. P.: Benthic and Pelagic Pathways of Methylmercury Bioaccumulation in Estuarine Food Webs of the Northeast United States, PLOS ONE, 9, e89 305, https://doi.org/10.1371/JOURNAL.PONE.0089305, 2014.

Cibic, T., Baldassarre, L., Cerino, F., Comici, C., Fornasaro, D., Kralj, M., and Giani, M.: Benthic and Pelagic Contributions to Primary Production: Experimental Insights From the Gulf of Trieste (Northern Adriatic Sea), Frontiers in Marine Science, 9, https://doi.org/10.3389/fmars.2022.877935, 2022.

Cossa, D. and Tabard, A.-M.: Mercury in Marine Mussels from the St. Lawrence Estuary and Gulf (Canada): A Mussel Watch Survey Revisited after 40 Years, Applied science, 10, 7556, https://doi.org/10.3390/app10217556, 2020.

da Silva, J. K. L., Garcia, G. J., and Barbosa, L. A.: Allometric scaling laws of metabolism, Physics of Life Reviews, 3, 229–261, https://doi.org/10.1016/J.PLREV.2006.08.001, 2006.

Daewel, U. and Schrum, C.: Low-frequency variability in North Sea and Baltic Sea identified through simulations with the 3-D coupled physical-biogeochemical model ECOSMO, Earth System Dynamics, 8, 801–815, https://doi.org/10.5194/esd-8-801-2017, 2017.

Daewel, U., Schrum, C., and MacDonald, J. I.: Towards end-to-end (E2E) modelling in a consistent NPZD-F modelling framework (ECOSMO E2E-v1.0): Application to the North Sea and Baltic Sea, Geoscientific Model Development, 12, 1765–1789, https://doi.org/10.5194/gmd-12-1765-2019, 2019.

Dijkstra, J. A., Buckman, K. L., Ward, D., Evans, D. W., Dionne, M., and Chen, C. Y.: Experimental and Natural Warming Elevates Mercury Concentrations in Estuarine Fish, PLOS ONE, 8, e58 401, https://doi.org/10.1371/JOURNAL.PONE.0058401, 2013.

Dufour, S. C.: Bivalve Chemosymbioses on Mudflats, Mudflat Ecology, pp. 169–184, https://doi.org/10.1007/978-3-319-99194-8_7, 2018.

https://doi.org/10.5194/egusphere-2025-1494
Preprint. Discussion started: 24 April 2025

Durnford, D., Dastoor, A., Figueras-Nieto, D., and Ryjkov, A.: Long range transport of mercury to the Arctic and across Canada, Atmos. Chem. Phys, 10, 6063–6086, https://doi.org/10.5194/acp-10-6063-2010, 2010.

Dutton, J. and Fisher, N. S.: Bioavailability of sediment-bound and algal metalsto killifish Fundulus heteroclitus, Aquatic biology, 16, 85–96, 2012.

Egbert, G. D. and Erofeeva, S. Y.: Efficient Inverse Modeling of Barotropic Ocean Tides, Journal of Atmospheric and Oceanic Technology, 19, 183–204, https://doi.org/10.1175/1520-0426(2002)019<0183:EIMOBO>2.0.CO;2, 2002.

English, M. D., Robertson, G. J., and Mallory, M. L.: Trace element and stable isotope analysis of fourteen species of marine invertebrates from the Bay of Fundy, Canada, Marine Pollution Bulletin, 101, 466–472, https://doi.org/10.1016/J.MARPOLBUL.2015.09.046, 2015.

Evers, D. C., Egan Keane, S., Basu, N., and Buck, D.: Evaluating the effectiveness of the Minamata Convention on Mercury: Principles and recommendations for next steps, https://doi.org/10.1016/j.scitotenv.2016.05.001, 2016.

Fox, A. L., Hughes, E. A., Trocine, R. P., Trefry, J. H., Schonberg, S. V., Mctigue, N. D., Lasorsa, B. K., Konar, B., and Cooper, L. W.: Mercury in the northeastern Chukchi Sea: Distribution patterns in seawater and sediments and biomagnification in the benthic food web, https://doi.org/10.1016/j.dsr2.2013.07.012, 2013.

Garcia H.E., Boyer T.P., Baranova O.K., Locarnini R.A., Mishonov A.V., Grodsky A., Paver C.R., Weathers K.W., Smolyar I.V., Reagan J.R., Seidov D., and Zweng M.W.: World Ocean Atlas 2018: Product Documentation. A. Mishonov, Technical Editor., 2019.

GEBCO Bathymetric Compilation Group: The GEBCO_2020 Grid - a continuous terrain model of the global oceans and land., Tech. rep., https://doi.org/https://doi.org/10.5285/a29c5465-b138-234d-e053-6c86abc040b9, 2020.

Gente`, S., Minet, A., Lopes, C., Tessier, E., Gassie, C., Guyoneaud, R., Swarzenski, P. W., Bustamante, P., Metian, M., Amouroux, D., and Lacoue-Labarthe, T.: In Vivo Mercury (De)Methylation Metabolism in Cephalopods under Different pCO 2 Scenarios, Cite This: Environ. Sci. Technol, 57, 5770, https://doi.org/10.1021/acs.est.2c08513, 2023.

Ghodrati Shojaei, M., Gutow, L., Dannheim, J., Rachor, E., Schröder, A., and Brey, T.: Common trends in German Bight benthic macrofaunal communities: Assessing temporal variability and the relative importance of environmental variables, Journal of Sea Research, 107, 25–33, https://doi.org/10.1016/j.seares.2015.11.002, 2016.

Gorokhova, E., Soerensen, A. L., and Motwani, N. H.: Mercury-methylating bacteria are associated with copepods: A proof-of-principle survey in the Baltic Sea, PLoS ONE, 15, https://doi.org/10.1371/journal.pone.0230310, 2020.

Haitzer, M., Aiken, G. R., and Ryan, J. N.: Binding of mercury(II) to dissolved organic matter: the role of the mercury-to-DOM concentration ratio, Environmental science & technology, 36, 3564–3570, https://doi.org/10.1021/ES025699I, 2002.

Harada, M.: Minamata Disease: Methylmercury Poisoning in Japan Caused by Environmental Pollution, Critical Reviews in Toxicology, 25, 1–24, https://doi.org/10.3109/10408449509089885, 1995.

Jensen, S. and Jernelov, A.: Biological Methylation of Mercury in Aquatic Organisms, Nature, 223, 753–754, 1969.

Korejwo, E., Saniewska, D., Bełdowski, J., Balazy, P., and Saniewski, M.: Mercury concentration and speciation in benthic organisms from Isfjorden, Svalbard, Marine Pollution Bulletin, 184, 114 115, https://doi.org/10.1016/J.MARPOLBUL.2022.114115, 2022.

Krause-Jensen, D., Markager, S., and Dalsgaard, T.: Benthic and Pelagic Primary Production in Different Nutrient Regimes, Estuaries and Coasts, 35, 527–545, https://doi.org/10.1007/s12237-011-9443-1, 2012.

Lavoie, R. A., Hebert, C. E., Rail, J.-F., Braune, B. M., Yumvihoze, E., Hill, L. G., and Lean, D. R. S.: Trophic structure and mercury distribution in a Gulf of St. Lawrence (Canada) food web using stable isotope analysis, https://doi.org/10.1016/j.scitotenv.2010.07.053, 2010.

https://doi.org/10.5194/egusphere-2025-1494
Preprint. Discussion started: 24 April 2025

Lin, H., Ascher, D. B., Myung, Y., Lamborg, C. H., Steven, Hallam, J., Gionfriddo, C. M., Kathryn, Holt, E., and Moreau, J. W.: Mercury methylation by metabolically versatile and cosmopolitan marine bacteria, The ISME Journal, 15, 1810–1825, https://doi.org/10.1038/s41396-020-00889-4, 2021.

Lønborg, C., Carreira, C., Abril, G., Agustí, S., Amaral, V., Andersson, A., Arístegui, J., Bhadury, P., Bif, M. B., Borges, A. V., Bouillon, S., Calleja, M. L., Cotovicz, L. C., Cozzi, S., Doval, M., Duarte, C. M., Eyre, B., Fichot, C. G., García-Martín, E. E., Garzon-Garcia, A., Giani, M., Gonçalves-Araujo, R., Gruber, R., Hansell, D. A., Hashihama, F., He, D., Holding, J. M., Hunter, W. R., Ibánhez, J. S. P., Ibello, V., Jiang, S., Kim, G., Klun, K., Kowalczuk, P., Kubo, A., Lee, C. W., Lopes, C. B., Maggioni, F., Magni, P., Marrase, C., Martin, P., McCallister, S. L., McCallum, R., Medeiros, P. M., Morán, X. A. G., Muller-Karger, F. E., Myers-Pigg, A., Norli, M., Oakes, J. M., Osterholz, H., Park, H., Lund Paulsen, M., Rosentreter, J. A., Ross, J. D., Rueda-Roa, D., Santinelli, C., Shen, Y., Teira, E., Tinta, T., Uher, G., Wakita, M., Ward, N., Watanabe, K., Xin, Y., Yamashita, Y., Yang, L., Yeo, J., Yuan, H., Zheng, Q., and Álvarez-Salgado, X. A.: A global database of dissolved organic matter (DOM) concentration measurements in coastal waters (CoastDOM v1), Earth System Science Data, 16, 1107–1119, https://doi.org/10.5194/ESSD-16-1107-2024, 2024.

Madgett, A. S., Yates, K., Webster, L., McKenzie, C., and Moffat, C. F.: The concentration and biomagnification of trace metals and metalloids across four trophic levels in a marine food web, Marine Pollution Bulletin, 173, 112 929, https://doi.org/10.1016/j.marpolbul.2021.112929, 2021.

Mason, R. P., Reinfelder, J. R., and Morel, F. M.: Uptake, toxicity, and trophic transfer of mercury in a coastal diatom, Environmental Science and Technology, 30, 1835–1845, https://doi.org/10.1021/es950373d, 1996.

Metian, M., Pouil, S., Dupuy, C., Teyssié, J.-L., Warnau, M., and Bustamante, P.: Influence of food (ciliate and phytoplankton) on the trophic transfer of inorganic and methyl-mercury in the Pacific cupped oyster Crassostrea gigas, Environmental Pollution, 257, https://doi.org/10.1016/j.envpol.2019.113503ï, 2020.

Muhaya, B. B. M., Leermakers, M., and Baeyens, W.: Total mercury and methylmercury in sediments and in the polychaete nereis diversicolor at groot buitenschoor (scheldt estuary, belgium), Water, Air, and Soil Pollution, 94, 109–123, 1997.

Olinger, L. K., Strangman, W. K., McMurray, S. E., and Pawlik, J. R.: Sponges With Microbial Symbionts Transform Dissolved Organic Matter and Take Up Organohalides, Frontiers in Marine Science, 8, 665 789, https://doi.org/10.3389/FMARS.2021.665789/BIBTEX, 2021.

Orani, A. M., Vassileva, E., Azemard, S., and Thomas, O. P.: Comparative study on Hg bioaccumulation and biotransformation in Mediterranean and Atlantic sponge species, Chemosphere, 260, 127 515, https://doi.org/10.1016/J.CHEMOSPHERE.2020.127515, 2020.

Outridge, P. M., Mason, R. P., Wang, F., Guerrero, S., and Heimbürger-Boavida, L. E.: Updated Global and Oceanic Mercury Budgets for the United Nations Global Mercury Assessment 2018, https://doi.org/10.1021/acs.est.8b01246, 2018.

Pacyna, E. G., Pacyna, J. M., Steenhuisen, F., and Wilson, S.: Global anthropogenic mercury emission inventory for 2000, Atmospheric Environment, 40, 4048–4063, https://doi.org/10.1016/j.atmosenv.2006.03.041, 2006.

Pan, K. and Wang, W. X.: Mercury accumulation in marine bivalves: Influences of biodynamics and feeding niche, Environmental Pollution, 159, 2500–2506, https://doi.org/10.1016/J.ENVPOL.2011.06.029, 2011.

Polak-Juszczak, L.: Selenium and mercury molar ratios in commercial fish from the Baltic Sea: Additional risk assessment criterion for mercury exposure, https://doi.org/10.1016/j.foodcont.2014.10.046, 2014.

Polak-Juszczak, L.: Distribution of organic and inorganic mercury in the tissues and organs of fish from the southern Baltic Sea, Environmental Science and Pollution Research, 25, 34 181–34 189, https://doi.org/10.1007/s11356-018-3336-9, 2018.

https://doi.org/10.5194/egusphere-2025-1494
Preprint. Discussion started: 24 April 2025

Richardson, K., Bo, F., Richardson, P., Pedersen, B., and Richardson, K.: Estimation of new production in the North Sea: consequences for temporal and spatial variability of phytoplankton, Tech. rep., 1998.

Schartup, A. T., Qureshi, A., Dassuncao, C., Thackray, C. P., Harding, G., Sunderland, E. M., Harvard, and Paulson, J. A.: A Model for Methylmercury Uptake and Trophic Transfer by Marine Plankton, Environ. Sci. Technol, 52, 18, https://doi.org/10.1021/acs.est.7b03821, 2018.

Seelen, E., Liem-Nguyen, V., Wünsch, U., Baumann, Z., Mason, R., Skyllberg, U., and Björn, E.: Dissolved organic matter thiol concentrations determine methylmercury bioavailability across the terrestrial-marine aquatic continuum, Nature Communications, 14, https://doi.org/10.1038/s41467-023-42463-4, 2023.

Sheehan, M. C., Burke, T. A., Navas-Acien, A., Breysse, P. N., Mcgready, J., and Fox, M. A.: Systematic reviews Global methylmercury exposure from seafood consumption and risk of developmental neurotoxicity: a systematic review, Bull World Health Organ, 92, 254–269, https://doi.org/10.2471/BLT.12.116152, 2014.

Silberberger, M. J., Renaud, P. E., Kröncke, I., and Reiss, H.: Food-web structure in four locations along the European shelf indicates spatial differences in ecosystem functioning, Frontiers in Marine Science, 5, 300 569, https://doi.org/10.3389/FMARS.2018.00119/BIBTEX, 2018.

Sizmur, T., Canário, J., Gerwing, T. G., Mallory, M. L., and O'Driscoll, N. J.: Mercury and methylmercury bioaccumulation by polychaete worms is governed by both feeding ecology and mercury bioavailability in coastal mudflats, Environmental Pollution, 176, 18–25, https://doi.org/10.1016/J.ENVPOL.2013.01.008, 2013.

Sommar, J., Osterwalder, S., and Zhu, W.: Recent advances in understanding and measurement of Hg in the environment: Surface-atmosphere exchange of gaseous elemental mercury (Hg0), Science of The Total Environment, 721, 137 648, https://doi.org/10.1016/J.SCITOTENV.2020.137648, 2020.

Taylor, D. L., Linehan, J. C., Murray, D. W., and Prell, W. L.: Indicators of sediment and biotic mercury contamination in a southern New England estuary, Marine Pollution Bulletin, 64, 807–819, https://doi.org/10.1016/J.MARPOLBUL.2012.01.013, 2012.

Taylor, V. F., Buckman, K. L., Seelen, E. A., Mazrui, N. M., Balcom, P. H., Mason, R. P., and Chen, C. Y.: Organic carbon content drives methylmercury levels in the water column and in estuarine food webs across latitudes in the Northeast United States, Environmental Pollution, 246, 639–649, https://doi.org/10.1016/J.ENVPOL.2018.12.064, 2019.

Tsui, M. T. and Wang, W. X.: Uptake and Elimination Routes of Inorganic Mercury and Methylmercury in Daphnia magna, Environmental Science and Technology, 38, 808–816, https://doi.org/10.1021/es034638x, 2004.

Wang, W. and Wong, R.: Bioaccumulation kinetics and exposure pathways of inorganic mercury and methylmercury in a marine fish, the sweetlips Plectorhinchus gibbosus, Marine Ecology Progress Series, 261, https://doi.org/10.3354/meps261257, 2003.

Wouters, H., Berckmans, J., Maes, R., Vanuytrecht, E., and De Ridder, K.: Global bioclimatic indicators from 1979 to 2018 derived from reanalysis, version 1.0, Copernicus Climate Change Service (C3S) Climate Data Store (CDS), DOI: 10.24381/cds.bce175f0, 2021.

Zaferani, S. and Biester, H.: Mercury Accumulation in Marine Sediments – A Comparison of an Upwelling Area and Two Large River Mouths, Frontiers in Marine Science, 8, 732 720, https://doi.org/10.3389/FMARS.2021.732720/BIBTEX, 2021.

Zhao, C., Daewel, U., and Schrum, C.: Tidal impacts on primary production in the North Sea, Earth System Dynamics, 10, 287–317, https://doi.org/10.5194/esd-10-287-2019, 2019.